# A Macro- and Micro-Approach to the Anisotropic Fatigue Performance of Progressively Drawn Pearlitic Steel

**J. Toribio[1], J. C. Matos[2] and B. González[1]**

[1] Department of Materials Engineering, University of Salamanca, E.P.S. Zamora, Campus Viriato, Avda. Requejo 33, 49022 Zamora, Spain. e-mail: toribio@usal.es
[2] Department of Computing Engineering, University of Salamanca, E.P.S. Zamora, Campus Viriato, Avda. Requejo 33, 49022 Zamora, Spain. e-mail: jcmatos@usal.es

***ABSTRACT.*** *This paper analyzes the propagation of fatigue cracks in pearlitic steel in two materials, hot rolled bar and cold drawn wire. The experimental procedure consisted of fatigue tests on cylindrical bars under tensile loading, using steps with decreasing amplitude of stress and constant stress range during each step. Results show how the cold drawing process improves the fatigue behaviour of eutectoid steel by retarding the fatigue crack growth rate in the Paris regime. The fracto-metallographic analysis shows how the microstructural anisotropy of the drawn steel (consequence of the drawing process itself) creates a change in the fracture crack path in the form of local micro-deflections (and thus multiaxially-driven fatigue propagation at the very local microscale). The net fatigue surface increases with cold drawing due to the higher angle of crack micro-deflections in the case of the heavily drawn material, thereby allowing a correction of the Paris law curves by considering the real (experimental) fatigue crack path (multi-deflected; locally multiaxial) and the theoretical fatigue crack path (non deflected; locally uniaxial).*

## INTRODUCTION

The fatigue phenomenon is generally considered as a two-parameter problem [1-3] involving two crack-tip driving forces, $\Delta K$ and $K_{max}$. For ductile materials, the fatigue driving force is dominated by the $\Delta K$ parameter and for the brittle materials by $K_{max}$ [4].

The long crack growth can be described using the Paris-Erdogan law [5]. In fully pearlitic steels, the increase in the stress ratio $R$ (minimum to maximum applied stress) or the decrease in the test temperature (from room temperature to -125 °C), produce a significant increase in the slope of the Paris-Erdogan curve, a phenomenon that coincides with an increase in the amount of the static mode of fracture (i.e. cleavage) [6].

Although some authors maintain that the fatigue crack growth in the Paris region is not influenced by the microstructure [7,8], which can be attributed to the fact that the cyclic plastic zone size is greater than the size of the characteristic microstructural unit, it has been observed how cold drawing of pearlitic steel improves the fatigue behaviour in the form of a decrease of the Paris constant $C$ [9].

The fatigue cracking path is indeed determined by the microstructure. In ferritic-pearlitic steels the crack runs through the ferritic seam in the grain boundaries [10]. In steel with pearlite uniformly distributed in ferrite, the crack path is more tortuous than in those with isolated distribution, with larger angle deflections appearing along the cracking path [11]. In eutectoid steel with fully pearlitic microstructure, the crack has a preference for breaking the pearlite lamellae (producing a transcollonial fracture), presenting at the microscopic level frequent deflections along the crack path, branchings, bifurcations, changes in the crack opening and discontinuities [9].

In banded ferritic-pearlitic steels, the bands of pearlite (oriented in preferential directions) decreases the rate of fatigue crack growth, since it causes a more tortuous crack path, with a greater number of branchings and deflections, which also have larger angles [12]. The tortuous path induces a frequent crack interlock and the crack branching reduces the local crack tip driving forces for its propagation [12]. The pearlite lamellar orientation in fully pearlitic steels produces a retardation in the crack growth rate because the lamellae behave as serious obstacles for the crack propagation [9,13]. Furthermore, an increase in surface roughness of the fracture is produced [9], due to the increased angle and number of deflections in the cracking.

## EXPERIMENTAL PROCEDURE

The material was pearlitic steel, whose composition appears on Table 1, supplied in two forms: firstly, as a hot rolled bar which has not been cold drawn at all and, secondly, as a commercial cold drawn wire which has undergone seven steps of cold drawing and a thermo-mechanical treatment to eliminate (or at least relieve) residual stresses at its surface.

Table 1. Chemical composition (wt %) of the steel.

| % C | % Mn | % Si | % P | % Cr | % V |
|---|---|---|---|---|---|
| 0.789 | 0.681 | 0.210 | 0.010 | 0.218 | 0.061 |

The mechanical properties of both steels were obtained after a standard tension test. Table 2 shows the Young's modulus $E$, a factor that barely changes with the drawing process, the 0.2 % conventional yield strength $\sigma_Y$ and the tensile strength $\sigma_R$ (significantly increasing both with the drawing), and the strain at maximum load $\varepsilon_R$ (which decreases with the drawing).

Table 2. Mechanical properties of the steels.

| Steel | $E$ (GPa) | $\sigma_Y$ (GPa) | $\sigma_R$ (GPa) | $\varepsilon_R$ |
|---|---|---|---|---|
| Hot rolled bar | 202 | 0.70 | 1.22 | 0.08 |
| Cold drawn wire | 209 | 1.48 | 1.82 | 0.06 |

Transversal and longitudinal samples from each material form were cut, mounted, grounded and polished until a mirror surface was obtained. After being etched with 4 % Nital (mixture of 4 ml of nitric acid with 96 ml of ethanol) to reveal microstructure, they were examined by scanning electron microscopy (SEM) with magnification factor up to x6000.

In fatigue tests the specimens used were cylindrical bars of 300 mm of length, diameters of 11.0 mm and 5.1 mm for the hot rolled bar and for the cold drawn wire, respectively. Before the test, a small transversal cut was performed on the middle part of the specimens, so as to cause the crack initiation at this point. During the test, the applied load $F$, the extensometer displacement $u$ (placed on the specimen in a symmetric way to the crack front) and the number of cycles $N$, were recorded.

The test procedure consisted of applying an oscillating tensile loading in the axial direction in successive decreasing steps, with a constant stress range $\Delta\sigma$ during each step and decreasing value from one to another step. The frequency used was 10 Hz, with the shaped of a sinusoidal wave and $R$-ratios $\approx 0$. The initial maximal stress was always lower than the yield strength, decreasing in the next steps around 20÷30 % with regard to the maximal stress in the previous step. Every load step was maintained enough time to be able to appreciate the crack advance and eliminate the plastic effect at the crack tip caused by the previous step.

## EXPERIMENTAL RESULTS

### *Microstructural Analysis*

In Figs. 1 and 2 the microstructure is shown of both the hot rolled and the cold drawn steels, respectively, in their characteristic sections transverse and longitudinal. The horizontal side of the photograph is associated with the radial direction in the wire, whereas the vertical side of the photograph corresponds to the annular direction in the transverse section and to the axial direction in the longitudinal section.

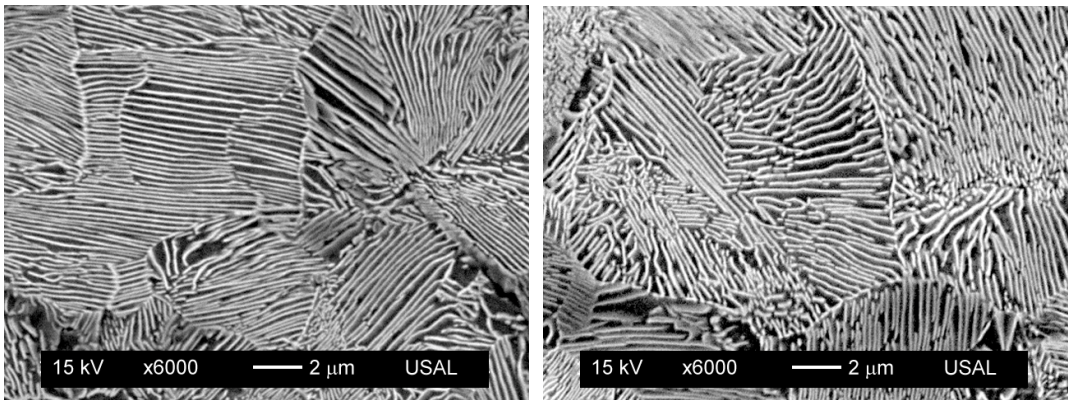


Figure 1. Microstructure of the hot rolled bar,
transversal section (left) and longitudinal section (right).

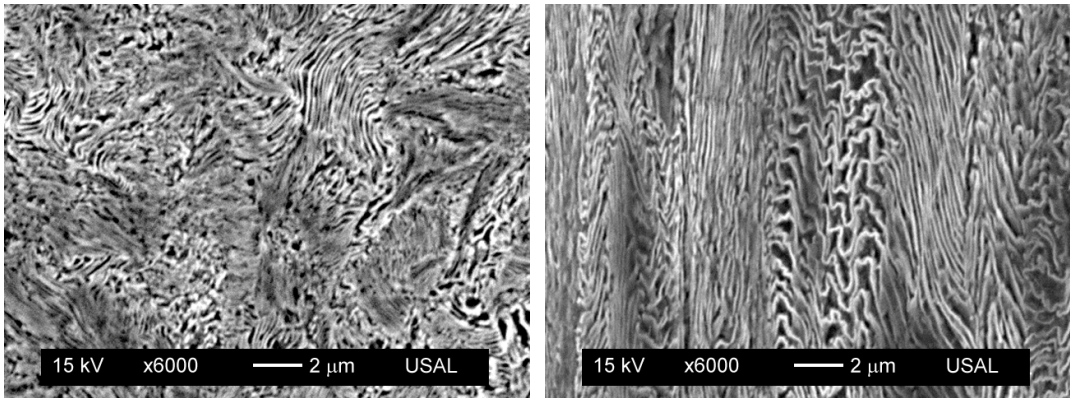


Figure 2. Microstructure of the cold drawn wire,
transversal section (left) and longitudinal section (right).

In a transverse section of the cold drawn steel, a random orientation and curling of both pearlitic colonies and lamellae is observed, together with an increasing packing closeness with cold drawing (i.e. the pearlite interlamellar spacing decreases with the drawing degree). On the other hand, in a longitudinal section of the same heavily drawn steel, the microstructural units evolve towards an oriented arrangement, becoming almost parallel to the wires axis or drawing direction. Such an orientation is associated with a longitudinal enlargement (with pearlite colonies slenderising) and a transverse shortening (and the afore-said increase of packing closeness and decrease of interlamellar spacing).

### *Fatigue Crack Growth*

After the tests, the fatigue fracture surfaces of the bars were observed. In both steels the fatigue surface was contained in the transverse section of the wire (perpendicular to the loading direction), thereby exhibiting mode I fracture even in the prestressing steel wire (heavily drawn) where a microstructural anisotropy does exist due to the cold drawing process. In every load change the crack front was modelled as part of an ellipse with centre on the bar surface, of semiaxes $a$ (crack depth) and $b$. In the central point of the crack front, where a plane strain state is achieved due to the enough constraint there, the curve representing the fatigue crack growth was calculated: cyclic crack growth rate $\mathrm{d}a/\mathrm{d}N$ versus stress intensity factor range $\Delta K$.

The value of the $\Delta K$ for the studied geometry, the crack size and the type of applied load, is:

$$\Delta K = Y \Delta\sigma \sqrt{\pi a} \tag{1}$$

where the used dimensionless stress intensity factor (SIF) $Y$ is that calculated by Astiz [14] for the central point of the crack.

Figure 3 plots the d$a$/d$N$-$\Delta K$ curve in the steady-state region (Paris regime) for both steels, the hot rolled bar and the cold drawn wire. The bilogarithmic fit is parallel for both steels (hot rolled bar and cold drawn wire) with the same slope, but the cold drawn wire curve appears down and to the left in relation to that of the hot rolled bar. Therefore, the cold drawn prestressing steel wire exhibits fatigue crack growth retardation in relation to the behaviour of the hot rolled bar, i.e., there is an improvement of fatigue performance in the former.

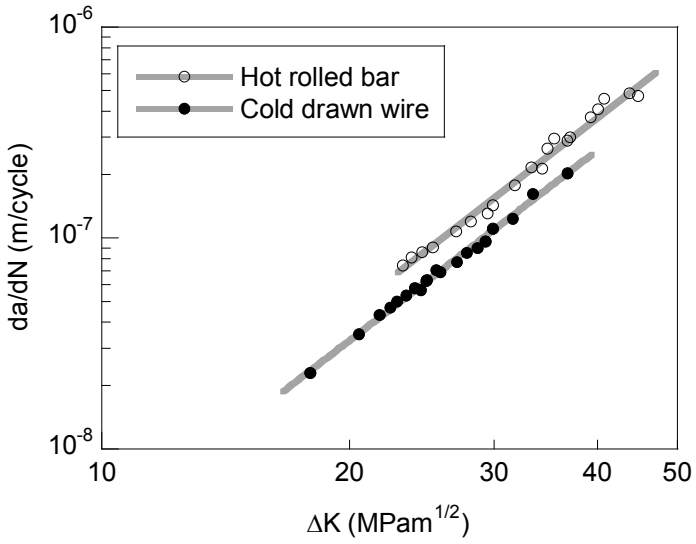


Figure 3. Paris curves for the hot rolled bar and the cold drawn wire.

From the adjustment of the data experimentially obtained to the Paris-Erdogan equation [5],

$$\frac{\mathrm{d}a}{\mathrm{d}N} = C\Delta K^{\mathrm{m}} \tag{2}$$

the parameters $C$ and $m$ of Paris are calculated (Table 3). The coefficient $m$ (slope of the straight line) remains constant and thus independent of the drawing process, while the constant $C$ decreases, being reduced by almost one quarter for an accumulated plastic deformation of 1.57 in the cold-drawn wire.

Table 3. Paris coefficients $C$ and $m$
(units for d$a$/d$N$ in m/cycle and $\Delta K$ in MPam$^{1/2}$).

| Steel | $C$ | $m$ |
|---|---|---|
| Hot rolled bar | $5.3\cdot10^{-12}$ | 3.0 |
| Cold drawn wire | $4.1\cdot10^{-12}$ | 3.0 |

***Fractomaterialography***

At microscopic level, the cracking presents in its path frequent deflections, branchings, bifurcations, changes in the crack opening and discontinuities [9]. For various ranges of the SIF, the profiles followed by the fatigue crack in the longitudinal sections of the specimen were drawn up (Fig. 4).

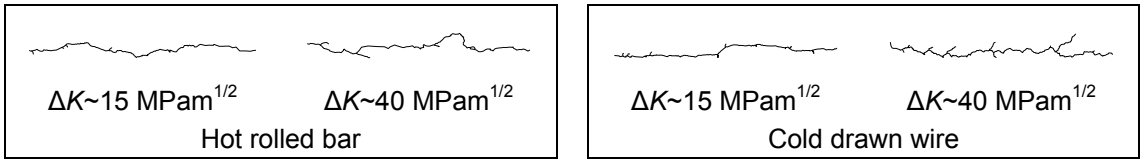


Figure 4. Fatigue crack profiles.

The profile length ratio $\lambda$ –ratio of the actual length of the crack increment, $l_r$, to the length of its transverse projection, $l_0$– was calculated,

$$\lambda = \frac{l_r}{l_0} \tag{3}$$

checking that its value increases with the stress intensity factor range, $\lambda=\lambda(\Delta K)$, as well as with the drawing process (Fig. 5).

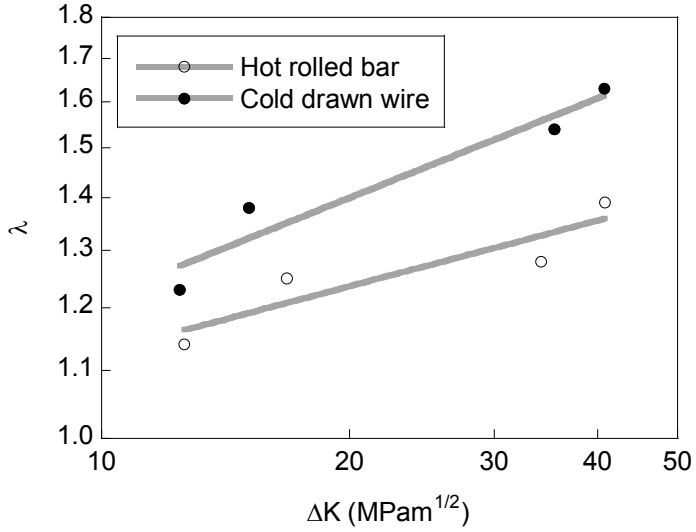


Figure 5. Profile length ratio, $\lambda$.

Although the fatigue fracture surface of the hot-rolled bar exhibits, at the meso level, cracking with greater height variations than the cold-drawn wire, at a finer micro-level the latter exhibits higher micro-roughness, so that the actual fractured surface in the cold-drawn wire is greater than that in the hot-rolled bar, and the crack deflection events are more frequent and with higher angle in the former (the drawn material).

## DISCUSSION

On the basis of previous results, a correction can be made in the cyclic crack growth rate by introducing the ratio of the actual cracked area $a_r$ to the projected one $a$ (which is that usually appearing in the Paris law), yielding the expression:

$$\frac{da_r}{dN} = \lambda \frac{da}{dN} \tag{4}$$

Figure 6 shows the "corrected" Paris law $da_r/dN$-$\Delta K$ in a bilogarithmic plot, where the lines of the two steels have moved up and the distance between them has been reduced, with the slope also increasing slightly.

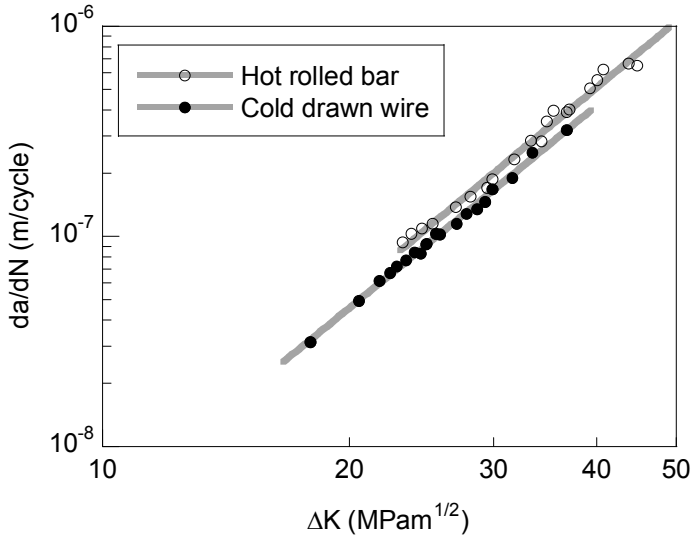


Figure 6. Modified Paris curves for the hot rolled bar and the cold drawn wire.

The fitting of the new experimental data (taking into account the actual cracked area), to the corrected Paris-Erdogan equation, allows one to obtain the modified Paris coefficients (Table 4).

$$\frac{da_r}{dN} = C_r \Delta K^{m_r} \tag{5}$$

Table 4. Modified Paris coefficients $C_r$ and $m_r$ (units for $da/dN$ in m/cycle and $\Delta K$ in MPam$^{1/2}$).

| Steel | $C_r$ | $m_r$ |
|---|---|---|
| Hot rolled bar | $3.3 \cdot 10^{-12}$ | 3.2 |
| Cold drawn wire | $3.2 \cdot 10^{-12}$ | 3.2 |

The results show how the manufacturing process, cold drawing, is beneficial from the standpoint of the resistance of pearlitic steels to cyclic stresses (because it improves their

response, enlarging their fatigue life), which can largely be attributed to the increase in the net fractured surface (micro-roughness) in the drawn steel.

## CONCLUSIONS

(i) The drawing of pearlitic steel improves its fatigue behaviour and produces a crack growth retardation. The Paris curve of the cold drawn wire is parallel to that of the hot rolled bar, but it is located beneath it.
(ii) The fatigue fracture surface of the drawn steel shows micro-roughness with greater net surface than in the rolled material due to the fact that the deflections in the fatigue path are more frequent and with greater angle.
(iii) A modification of the Paris law was proposed in the paper, consisting of using the actual fatigue fracture surface instead of the transverse projection of it. After that correction, the Paris curves of both steels (hot rolled bar and cold drawn wire) become closer.

## ACKNOWLEDGEMENTS

The authors wish to acknowledge the financial support provided by the following Spanish Institutions: MCYT (Grant MAT2002-01831), MEC (Grant BIA2005-08965), MICINN (Grants BIA2008-06810 and BIA2011-27870), and JCyL (Grants SA067A05, SA111A07, and SA039A08), and the steel supplied by EMESA TREFILERÍA (La Coruña, Spain).

## REFERENCES

1. Sadananda, K., Vasudevan, A.K. (2004) *Int. J. Fatigue* **26**, 39-47.
2. Stoychev, S., Kujawski, D. (2005) *Int. J. Fatigue* **27**, 1425-1431.
3. Zhang, J., He, X.D., Du, S.Y. (2005) *Int. J. Fatigue* **27**, 1314-1318.
4. Kujawski, D. (2001) *Int. J. Fatigue* **23**, S239-S246.
5. Paris, P.C., Erdogan, F. (1963) *J. Basic Eng.* **85D**, 528-534.
6. El-Shabasy, A.B., Lewandowski, J.J. (2004) *Int. J. Fatigue* **26**, 305-309.
7. Subramanya Sarma, V., Padmanabhan, K.A., Jaeger, G., Koethe, A., Schaper, M. (2000) *Mater. Lett.* **46**, 185-188.
8. Sankaran, S., Subramanya Sarma, V., Padmanabhan, K.A., Jaeger, G., Koethe, A. (2003) *Mater. Sci. Eng.* **A362**, 249-256.
9. Toribio, J., Matos, J.C., González, B. (2009) *Int. J. Fatigue* **31**, 2014-2021.
10. Walther, F., Eifler, D. (2004) *Mater. Sci. Eng.* **A387-389**, 481-485.
11. Korda, A.A., Mutoh, Y., Miyashita, Y., Sadasue, T. (2006) *Mater. Sci. Eng.* **A428**, 262-269.
12. Korda, A.A., Mutoh, Y., Miyashita, Y., Sadasue, T., Mannan, S.L. (2006) *Scripta Mater.* **54**, 1835-1840.
13. Wetscher, F., Stock, R., Pippan, R. (2007) *Mater. Sci. Eng.* **A445-446**, 237-243.
14. Astiz, M.A. (1986) *Int. J. Fracture* **31**, 105-124.